Genes Genet. Syst. (2025) **100**, 24-00110

Transposition of the heat-activated retrotransposon *ONSEN* results in enhanced hypocotyl elongation

Ryu Hasegawa[1] and Hidetaka Ito[2*]

[1] *Graduate School of Life Science, Hokkaido University, Sapporo, Hokkaido 060-0810, Japan*
[2] *Faculty of Science, Hokkaido University, Sapporo, Hokkaido 060-0810, Japan*

(Received 31 May 2024, accepted 19 January 2025; J-STAGE Advance published date: 25 January 2025)

We aimed to identify new mutants resulting from *ONSEN* transposition in *Arabidopsis thaliana* by subjecting *nrpd1* mutant seedlings to heat stress. We isolated a mutant with a significantly elongated hypocotyl, named *Long hypocotyl in ONSEN-inserted line 1* (*hyo1*). This phenotype was heritable, with progeny consistently displaying longer hypocotyls than the wild type. Genetic analysis revealed that this trait was due to a single recessive mutation. Further mapping and sequencing identified the insertion of *ONSEN* into the *HY2* gene, a crucial regulator of hypocotyl elongation. The insertion disrupted *HY2* transcription, as confirmed by quantitative PCR, leading to the observed phenotype. To assess any influence of the *nrpd1* background, we generated lines backcrossed twice to wild-type Col-0, and the results were consistent with those observed in the original mutant lines. Furthermore, we examined the effect of *HY2* and *HYO1* mutations on flowering time by analyzing the expression levels of *FT*. The *hyo1* mutant exhibited earlier flowering compared to both wild type and the *nrpd1* mutant, with increased *FT* expression levels. This research highlights the impact of *ONSEN* transposition on gene function and phenotypic variation in *A. thaliana*, providing new insights into the mutagenic potential of transposons and their role in shaping plant traits.

Key words: *Arabidopsis thaliana*, heat stress, *ONSEN*, *HY2*, transposon

INTRODUCTION

Transposons make up a large portion of the genomes of plants and animals, and their transposition is one of the driving forces behind the genome evolution of organisms (Kazazian, 2004; Biémont and Vieira, 2006; Bucher et al., 2012; Casacuberta and González, 2013; Fultz et al., 2015). Transposons can be classified into Class I and Class II (Wicker et al., 2007). Class I, also called retrotransposons, is transposed in a "copy & paste" fashion. After synthesizing mRNA, retrotransposons synthesize a cDNA by reverse transcription. The cDNA intermediate is called extrachromosomal DNA; it inserts into a new chromosomal location, thereby increasing the copy number (Bucher et al., 2012). Class II, on the other hand, is called DNA-type transposons and is transposed in a "cut & paste" fashion (Sahebi et al., 2018). Compared to DNA-type transposons, retrotransposon copy number can potentially explode and alter the structure of the host genome.

Transposons are ubiquitous in the genomes of all organisms, yet the majority remain inactive. This inactivity stems partly from accumulated deletions or mutations within their DNA sequences, which render them non-functional. Additionally, host organisms typically repress transposon gene expression through epigenetic modifications, effectively silencing these mobile genetic elements (Wierzbicki et al., 2008; Gao et al., 2010).

Most transposons are repressed in expression, but some are known to be transiently activated by environmental stress (Lisch, 2009; Ito, 2022). *ONSEN*, a heat-activated retrotransposon, resides within the Arabidopsis genome. It features a heat shock element within its long terminal

Edited by Tetsu Kinoshita
* Corresponding author. hito@sci.hokudai.ac.jp
DOI: https://doi.org/10.1266/ggs.24-00110

repeat sequence, which is recognized as a binding site by the heat shock transcription factor HsfA2. This interaction triggers *ONSEN* activation at 37 °C (Cavrak et al., 2014). In the wild type, transposition of *ONSEN* is suppressed by an epigenetic mechanism called RNA-directed DNA methylation (RdDM) (Wierzbicki et al., 2008; Gao et al., 2010). In the RdDM pathway, small interfering RNA is synthesized by RNA polymerase IV (Pol IV) and forms an RNA-induced silencing complex that eventually recruits DNA methyltransferases, leading to *de novo* methylation of target TEs (Matzke and Birchler, 2005). However, when mutants of the RdDM pathway are exposed to heat, transgenerational transpositions of *ONSEN* are observed (Ito et al., 2011; Matsunaga et al., 2012).

Transposons can alter gene expression and phenotype by integrating into or near target genes. Transgenerational transposition of *ONSEN* can be triggered in the *nrpd1* mutant, which encodes the largest subunit of Pol IV, by subjecting it to heat stress at 37 °C for 24 h (Ito et al., 2011; Matsunaga et al., 2012). Previous studies have found that *ONSEN* preferentially targets euchromatic regions and affects gene expression (Ito et al., 2016). It has been reported that ABA stress-tolerant mutants were obtained from the *ONSEN*-inserted population in *nrpd1* (Ito et al., 2016). The insertion of *ONSEN* into ABA-responsive genes such as *ABI4* and *ABI5* can generate mutants that are insensitive to ABA stress. This demonstrates that *ONSEN* transposition can confer environmental adaptation to the host plant, highlighting its role in enhancing stress resilience through genetic modification.

In this paper, we present the discovery of a mutant displaying abnormal hypocotyl elongation, attributed to *ONSEN* transposition triggered by heat stress.

RESULTS

Characterization of a mutant in *ONSEN* insertion lines To identify novel mutants resulting from *ONSEN* transposition, we conducted a phenotypic analysis on a population of *ONSEN*-inserted lines generated by subjecting *nrpd1* mutants to heat stress. This screening led to the isolation of a mutant exhibiting significantly elongated hypocotyls compared to the wild type, which we designated as *Long hypocotyl in ONSEN-inserted line 1* (*hyo1*). To verify the heritability of this trait, seeds were collected from *hyo1* and grown. All progeny displayed the same elongated hypocotyl phenotype. At 5 days post-germination on vertical medium, the average hypocotyl length of the mutant was 10.11 mm, markedly longer than the 2.01 mm observed in wild-type plants. In comparison, the hypocotyl length of the original *nrpd1* mutant line used to create the *ONSEN*-inserted population averaged 2.16 mm (Fig. 1A and 1B).

***hyo1* has a recessive phenotype** To identify the genetic factor responsible for the elongated hypocotyls, the *hyo1* mutant was crossed with a wild-type L*er* accession. All F1 progeny exhibited the wild-type phenotype, indicating that the *hyo1* trait is recessive. In the F2 generation, approximately one-fourth of the seedlings displayed the elongated hypocotyl phenotype, suggesting that the trait is controlled by a single genetic locus (Fig. 2A).

The elongated hypocotyl phenotype in *hyo1* is independent of a mutation in *NRPD1* Given that *hyo1* originates from an *nrpd1* mutant background, we asked whether the elongated hypocotyl phenotype in *hyo1* could be attributed to the *nrpd1* mutation. While Figure 1 shows hypocotyl length in the *nrpd1* mutant alone, we further investigated the *nrpd1* mutation within the *hyo1* background by genotyping 16 F2 individuals from an *nrpd1*/L*er* cross, focusing specifically on long hypocotyl segregants. This analysis revealed six individuals homozygous for the *nrpd1* mutation, seven heterozygous, and three homozygous for the wild type (Fig. 2B). These results indicate that the *nrpd1* mutation is not responsible for the extended hypocotyl phenotype observed in *hyo1*.

Mapping of the gene responsible in *hyo1* To identify the gene responsible for the elongated hypocotyl phenotype, we conducted rough mapping using Col-0/L*er*

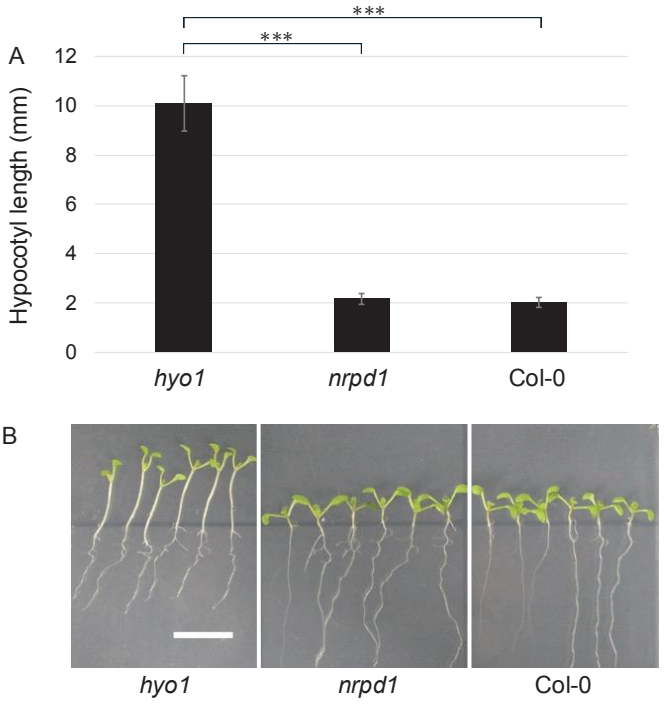

Fig 1. (A) Hypocotyl length measured 5 days after germination, showing the average length in 18–24 seedlings. Error bars represent the standard deviation (± SD). Statistical significance was determined using one-way analysis of variance (ANOVA) followed by Tukey's HSD test (***$P < 0.001$). (B) Seedlings 5 days after germination. Scale bar, 10 mm.

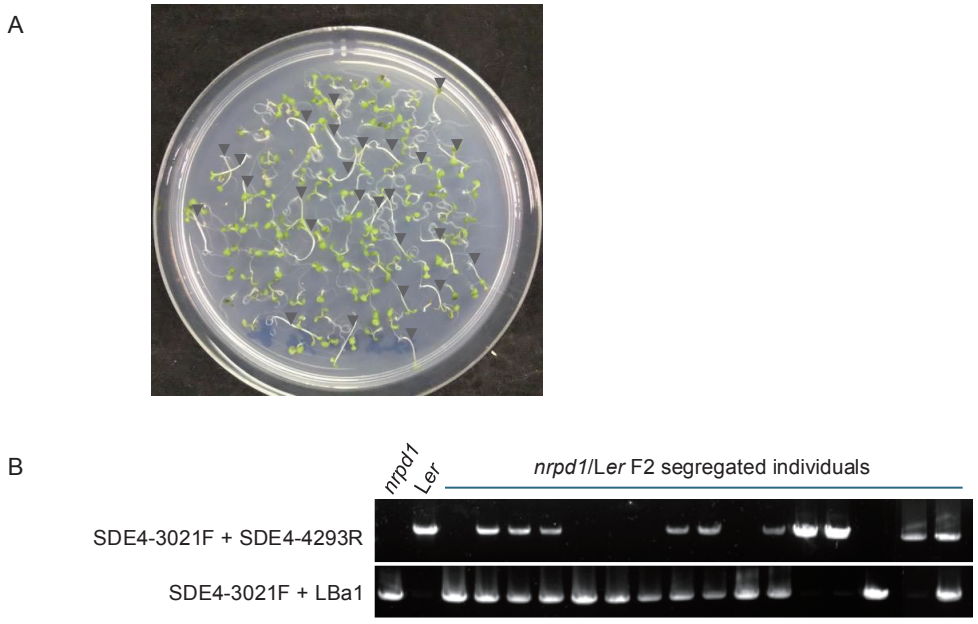

Fig. 2. (A) Phenotypes of F2 seedlings 5 days after germination from the cross between *hyo1* and L*er*. Among 117 individuals, 26 exhibited hypocotyl elongation (indicated by black arrowheads). (B) Genotyping results for the *nrpd1* mutation in the F2 population from the cross between *hyo1* and L*er*. Six individuals were homozygous for the *nrpd1* mutation, seven were heterozygous, and three were homozygous for the wild-type allele. All individuals used in this analysis were selected based on their elongated hypocotyls obtained from the segregating F2 population.

genetic markers across all five Arabidopsis chromosomes. Initially, we established one marker per chromosome and genotyped DNA samples from 16 F2 individuals. The analysis revealed that the genetic marker NGA162 on chromosome 3 was consistently associated with the Col-0 genotype in all samples, suggesting that the gene responsible is in this region. Further genotyping of 28 F2 DNA samples showed a 27:1 ratio of Col-0 homozygotes to Col-0/L*er* heterozygotes for markers NGA172 and NGA162, positioned at 786,296 bp and 4,608,277 bp on chromosome 3, respectively. These findings indicate that the gene responsible for the longer hypocotyl phenotype is situated near these markers on chromosome 3.

***ONSEN* is inserted in the *HY2* gene** The *ELONGATED HYPOCOTYL 2* (*HY2*) gene is situated at 2,803,597–2,805,588 bp, between the genetic markers on chromosome 3. *HY2* encodes the principal synthase for PϕB, a crucial cofactor for the photoreceptor phytochrome, and its disruption leads to hypocotyl elongation. In the *hy2* mutant, a T-DNA insertion is situated at 472 bp within the *HY2* gene (Fig. 3A). PCR analysis, using primers targeting the ends of the *HY2* gene, revealed a much larger DNA fragment in *hyo1* mutants compared to wild type (approximately 8 kb versus 3 kb, respectively) (Fig. 3B). This suggests the insertion of *ONSEN* within the *HY2* gene region. Further PCR analysis, using primers specific to both the *HY2* and *ONSEN* regions, was performed around the 5′ and 3′ junctions. On the 3′ side, this yielded a 1-kb fragment (Fig. 3C), which was confirmed by sequencing to be a fusion of *HY2* and *ONSEN* sequences (Supplementary Fig. S1). Similarly, analysis of the 5′ junction revealed a comparable fusion of *HY2* and *ONSEN* sequences. Segments of nucleotides matched both *HY2* and *ONSEN*, pinpointing the insertion at 1,408 bases within *HY2* (Fig. 3A).

To confirm that *HY2* disruption was responsible for the hypocotyl elongation phenotype, a complementation test was performed. F1 hybrids from crosses between *hyo1* and *hy2* mutants displayed significantly elongated hypocotyls compared to the wild type (Fig. 4A and 4B). These results clearly demonstrate that the insertion of *ONSEN* into the *HY2* gene disrupts its function, leading to the observed phenotype in *hyo1*.

The transcript of *HY2* is disrupted by the *ONSEN* insertion To assess the impact of *ONSEN* insertion on *HY2* gene transcription in *hyo1*, we performed quantitative PCR to measure transcript levels downstream of the insertion site. The results revealed a marked reduction in *HY2* transcripts in *hyo1* compared to both wild type and the control *nrpd1* mutant. Similarly, the *hy2* mutant, used as a control, also exhibited low levels of *HY2* transcripts. These findings indicate that the elongated hypocotyl phenotype in *hyo1* is attributable to the disrupted production of *HY2* gene transcripts (Fig. 4C).

Comparative analysis of hypocotyl length phenotypes in *hyo1* and related mutants To investigate whether the genetic background, specifically

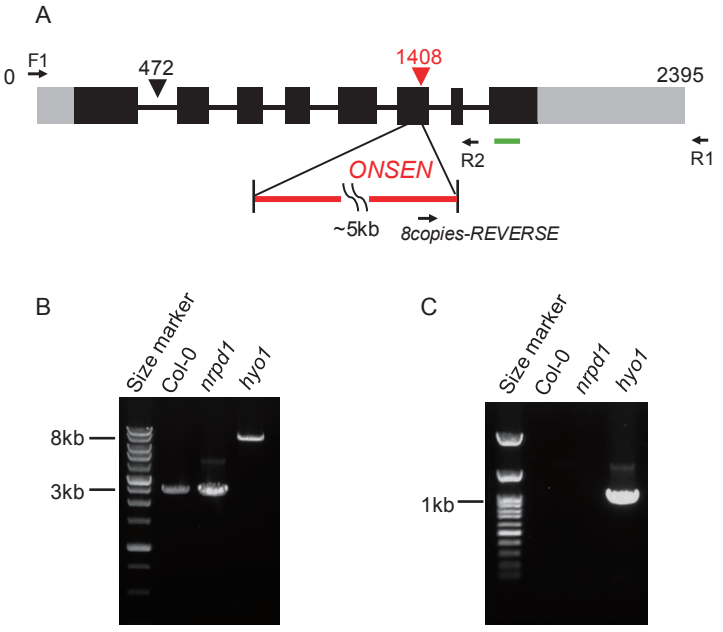

Fig. 3. (A) Gene structure of *HY2* and the insertion region of *ONSEN*. Gray rectangles indicate UTRs, black rectangles indicate exons, and lines indicate introns. The black arrowhead indicates the T-DNA insertion position of the Salk line (*SALK_104923C*), and the red arrowhead indicates the *ONSEN* insertion position. The numbers indicate the number of bases. The green line indicates the region examined by qRT-PCR. Arrows indicate the positions of primers used in the PCR reactions shown in (B) and (C). (B) PCR to distinguish *hyo* type from wild type using primers (F1 and R1) corresponding to sequences at both ends of the *HY2* gene. (C) PCR to confirm the presence of *ONSEN* using primers (8copies-REVERSE and R2) corresponding to the *HY2* and *ONSEN* regions.

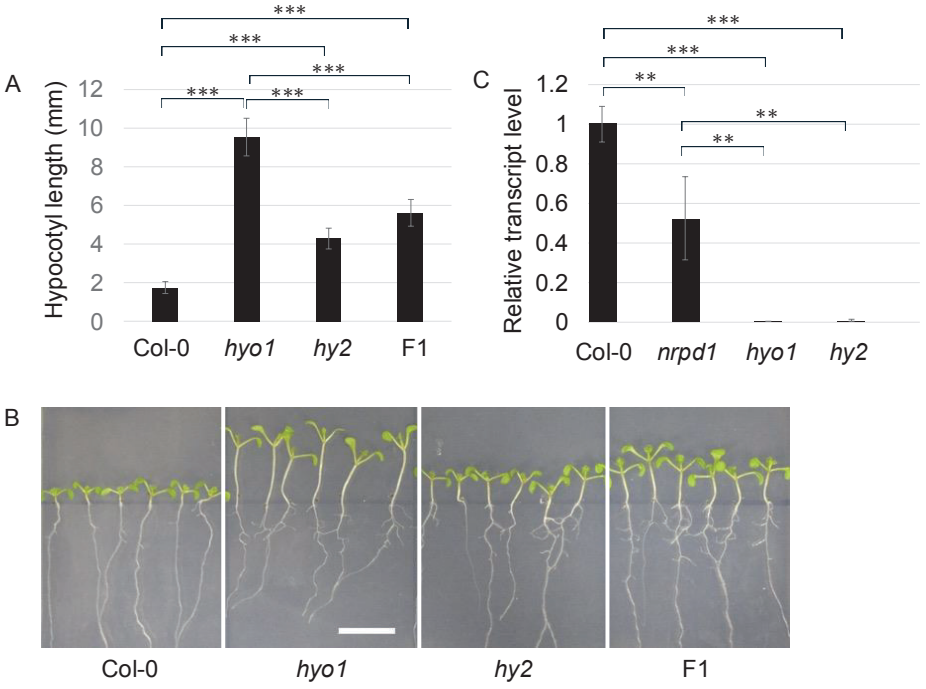

Fig. 4. (A) Hypocotyl length of seedlings 5 days after germination. Statistical significance was determined using one-way ANOVA followed by Tukey's HSD test (***$P < 0.001$). (B) Phenotypes of seedlings. F1: F1 hybrid of *hyo1* and *hy2*. Scale bar, 10 mm. (C) Relative transcript levels of the *HY2* gene relative to wild-type Col-0 in seedlings 7 days after germination. Error bars represent ± SD. Statistical significance was determined using one-way ANOVA followed by Tukey's HSD test (***$P < 0.001$, **$P < 0.01$).

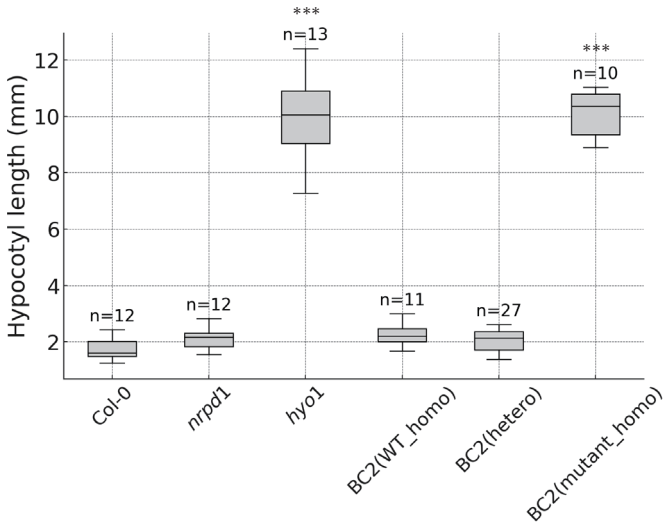

Fig. 5. Hypocotyl length of seedlings 5 days after germination. *n* indicates the number of individuals examined. BC2 (WT_homo or hetero) represents segregating populations from two backcrosses of *hyo1* with Col-0, where the *HY2* locus was either wild-type or heterozygous for the mutation. BC2 (mutant_homo) represents individuals homozygous for the mutation. Statistical significance was determined using one-way ANOVA followed by Tukey's HSD test (***$P < 0.001$, compared to Col-0).

the *nrpd1* mutation, influences hypocotyl length in the *hyo1* mutant, we backcrossed the *hyo1* mutant to the wild-type Col-0 background twice to eliminate any potential effects of the *nrpd1* mutation. Hypocotyl length analysis of progeny from these backcrossed plants revealed that, among 48 individuals, 38 displayed the short hypocotyl length typical of the wild type, while 10 exhibited the elongated hypocotyl phenotype characteristic of the *hyo1* mutant. Notably, all 10 individuals with elongated hypocotyls were homozygous mutants with an *ONSEN* insertion in the *HY2* gene, while the 38 individuals with short hypocotyls were either wild type or heterozygous at the *HY2* locus (Fig. 5). Furthermore, all 48 individuals were confirmed to have reverted to the wild-type genotype at the *NRPD1* locus. These results indicate that the elongated hypocotyl phenotype observed in *hyo1* mutants is independent of the *nrpd1* mutation and is associated with the *ONSEN* insertion in the *HY2* gene.

The *hyo1* mutant has an earlier flowering time To determine if the elongated hypocotyl of the *hyo1* mutant influences its flowering time, we compared the flowering times of wild type and *hyo1* and *nrpd1* mutants. The results revealed that *hyo1* mutants flowered significantly earlier, at 16 days after germination, compared to the wild type, which flowered at an average of 24 days. The *nrpd1* mutants, used as a control, took 29 days to flower, while the *hy2* mutants flowered in 21 days (Fig. 6A). Additionally, we assessed the relationship between flowering time and the number of rosette leaves. The wild type averaged 13 rosette leaves, the *nrpd1* mutants averaged 17, and the *hyo1* mutants averaged only 4, confirming an early flowering phenotype in *hyo1* (Fig. 6B). Notably, the *hyo1* mutants flowered even earlier than the *hy2* mutants (Fig. 6A and 6C). To examine whether the genetic background, particularly the *nrpd1* mutation, influences the flowering time of the *hyo1* mutant, the *hyo1* mutant was backcrossed twice to a wild-type Col-0 background to eliminate any potential effects of the *nrpd1* mutation. Flowering time analysis of progeny from these backcrosses, based on the number of rosette leaves at flowering, revealed that 39 out of 48 plants exhibited flowering times similar to the wild type, while nine plants displayed the early flowering phenotype characteristic of the *hyo1* mutant. Notably, all nine individuals with the early flowering phenotype were homozygous mutants carrying an *ONSEN* insertion in the *HY2* gene. In contrast, plants with flowering times comparable to the wild type were either wild type or heterozygous at the *HY2* locus (Fig. 6D). Additionally, all 48 individuals reverted to the wild-type genotype at the *NRPD1* locus. These findings indicate that the premature flowering phenotype observed in the *hyo1* mutant is independent of the *nrpd1* mutation and is associated with the *ONSEN* insertion in the *HY2* gene.

To investigate the cause of early flowering in *hyo1*, we focused on the role of the *FT* gene, a key regulator of flowering time. Since *FT* encodes the florigen that promotes flowering, we compared *FT* transcript levels between *hyo1* and wild-type plants using qRT-PCR. The results showed that *FT* expression was significantly higher in *hyo1* than in the wild type (Fig. 6E). This suggests that the early flowering phenotype of *hyo1* is attributable to increased *FT* transcript levels, potentially linking the elongated hypocotyls of *hyo1* to enhanced *FT* expression and accelerated flowering. Additionally, we analyzed samples from a segregating population of *hyo1* that had been backcrossed twice to Col-0. Among 48 individuals, *FT* transcript levels in the 39 plants with short hypocotyls were comparable to those of the wild type. In contrast, the nine plants with elongated hypocotyls exhibited significantly elevated *FT* transcript levels. Further genotyping revealed that the 39 plants with short hypocotyls were either wild type or heterozygous at the *HY2* locus, whereas all nine plants with elevated *FT* levels and elongated hypocotyls were homozygous mutants at the *HY2* locus, with an *ONSEN* insertion detected in the *HY2* gene (Fig. 6E). Additionally, all 48 individuals were verified to carry the wild-type genotype at the *NRPD1* locus. These findings suggest that the early flowering phenotype of *hyo1* is closely associated with elongated hypocotyls, which may be linked to the presence of the *ONSEN* insertion in the *HY2* locus, resulting in enhanced *FT* expression and accelerated flowering.

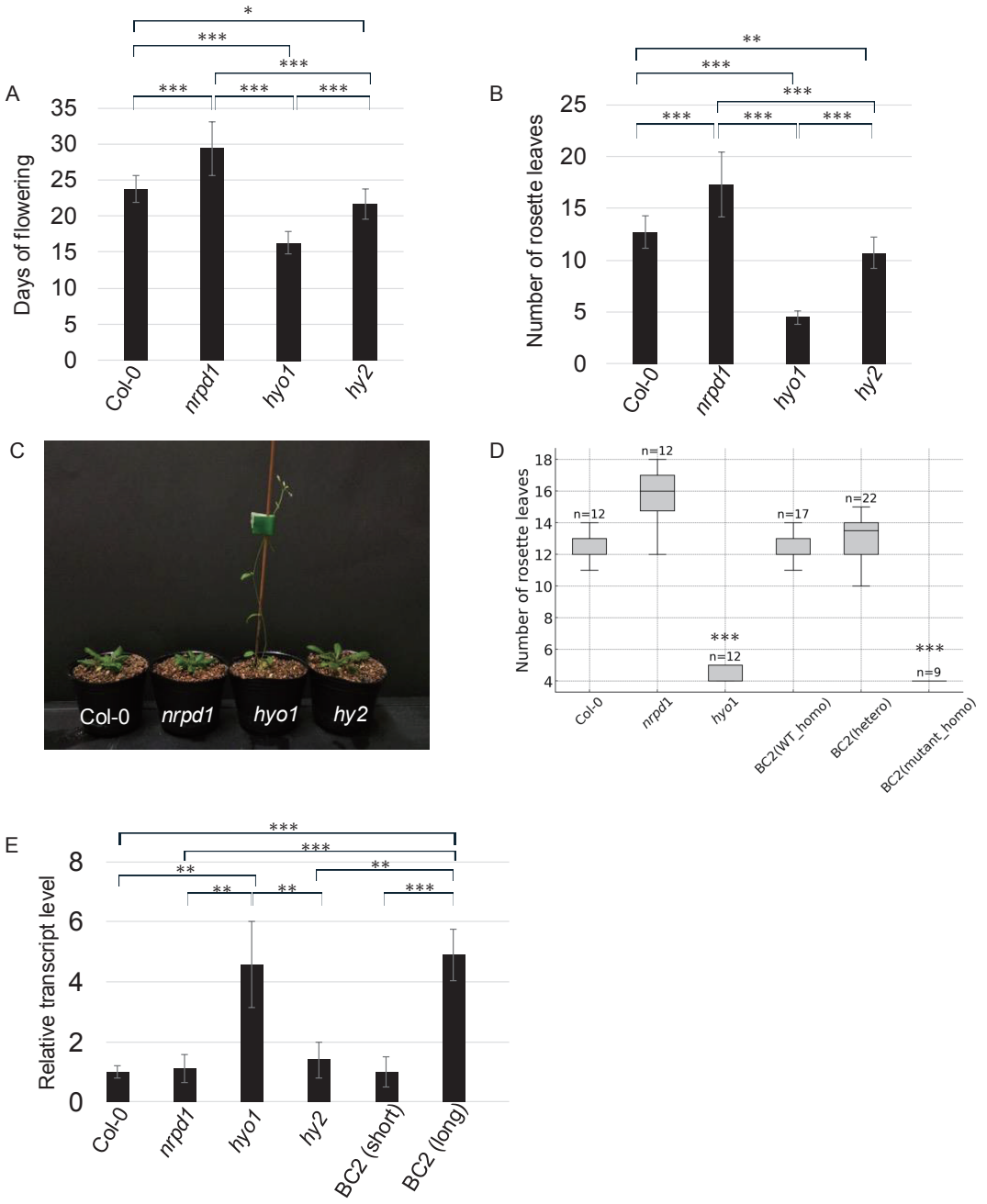

Fig. 6. Flowering time analysis was performed with 24 plants per group. (A) The number of days from germination to flowering. (B) Number of rosette leaves at bolting. (C) Early flowering phenotype in *hyo1*; representative plants were photographed 21 days after germination. (D) Number of rosette leaves at flowering time. *n* indicates the number of individuals examined. BC2 (WT_homo or hetero) refers to the population derived from two backcrosses between *hyo1* and Col-0, where the *HY2* locus was heterozygous for the wild type or mutation. BC2 (mutant_homo) refers to individuals homozygous for the mutation. Statistical significance was determined using one-way ANOVA followed by Tukey's HSD test (***$P < 0.001$, compared to Col-0). (E) qRT-PCR analysis of *FT* transcript levels. Data represent the mean of three biological replicates, with relative expression values normalized to WT (set as 1). BC2 (short) refers to individuals from a segregating population of *hyo1* backcrossed twice to Col-0 wild type, with short hypocotyls. BC2 (long) refers to individuals from the same population with elongated hypocotyls. Plants were analyzed at 8 days after germination. Error bars indicate ± SD. Statistical significance was determined using one-way ANOVA followed by Tukey's HSD test (*$P < 0.05$, **$P < 0.01$, ***$P < 0.001$).

DISCUSSION

New insertions of transposons generate a diverse array of traits and occasionally act as catalysts for evolutionary processes (Ito et al., 2016; Contreras-Garrido et al., 2024; He et al., 2024). In our previous research, we observed transgenerational transposition of *ONSEN* in *A. thaliana* mutants of the RdDM pathway under high-temperature stress (Ito et al., 2011). Building on this, we utilized the *nrpd1* mutant, a key RdDM pathway mutant, to screen *ONSEN*-inserted populations derived from heat-stressed progeny. Remarkably, we identified mutants exhibiting abnormally elongated hypocotyls. The hypocotyl elongation phenotype of *hyo1* is striking and distinguishable from the wild type just days after sowing. Subsequent genetic analysis indicated that this elongated hypocotyl phenotype is attributable to a mutation in a single gene. Classical mapping and sequencing identified an *ONSEN* insertion within the *HY2* gene. Consistent with previous findings that *ONSEN* preferentially inserts within genes, often targeting exons, our experiment revealed *ONSEN* integration into the sixth exon of the *HY2* gene. This demonstrates *ONSEN*'s potent capability to regulate gene expression.

Hypocotyl elongation in the *hyo1* mutant is even more pronounced than in the previously reported *hy2* mutant. This may be attributed to the different insertion sites of the T-DNA: while the *hy2* mutant has the insertion in the first intron, the *hyo1* mutant's *ONSEN* is inserted in the sixth exon of the *HY2* gene. Despite this difference, transcription analysis shows that both the *hy2* and *hyo1* mutants exhibit almost complete repression of the *HY2* gene. One potential explanation for the pronounced difference in hypocotyl elongation between the *hyo1* and *hy2* mutants could lie in their genetic backgrounds. The *hyo1* mutant was generated through the transposition of *ONSEN* within an *nrpd1* mutant background. Crucially, our data indicate that the elongated hypocotyl phenotype in *hyo1* is independent of the *nrpd1* mutation, as evidenced by the genotyping of F2 individuals. Although *nrpd1* is not directly responsible for the elongation phenotype, it might still exert some influence on hypocotyl length. To address this issue, we conducted multiple backcrosses of *hyo1* with the Col-0 wild type to restore the genetic background to that of the wild type. After backcrossing, we analyzed the segregating population to confirm that the elongated hypocotyl phenotype and early flowering trait persisted in the *hyo1* background, independent of other genetic influences introduced during the initial mutation process. This confirmed that the observed phenotypes are intrinsic to *hyo1* and not perceptibly influenced by residual genetic background effects.

Another possibility is that the insertion of *ONSEN* in the *hyo1* mutant disrupts nearby enhancer or promoter regions, leading to abnormal activation or suppression of *HY2* transcription or of the transcription of neighboring genes. Such changes in transcriptional regulation may contribute to the pronounced phenotypes observed in *hyo1* compared to *hy2*. Additionally, epigenetic modifications caused by the *ONSEN* insertion, such as altered DNA methylation or histone modifications, could influence the expression of *HY2* or other related genes. Since the *hyo1* mutant was originally generated in the *nrpd1* background, some of these epigenetic effects might have been retained even after multiple backcrosses, potentially contributing to the differences in hypocotyl elongation and flowering time between *hyo1* and *hy2*. Further investigation into the transcriptional and epigenetic landscapes surrounding the *ONSEN* insertion site in *hyo1* would help to elucidate these mechanisms.

The *hyo1* mutant exhibits markedly accelerated hypocotyl elongation, leading to an earlier flowering time. While the ecological advantages of this phenotype remain uncertain, it is plausible that the *ONSEN* transposition could drive genome evolution by modulating the flowering time in *A. thaliana*. This genetic alteration may provide a selective advantage under specific environmental conditions, potentially influencing the evolutionary trajectory of the species. Notably, the early flowering phenotype in *hyo1* is accompanied by a significant increase in *FT* expression, a key regulator of flowering time that encodes the florigen that promotes floral transition. This suggests that the *hyo1* mutation enhances the transcriptional activity of *FT*, potentially linking the mutant's accelerated flowering to the molecular regulation of this central flowering-time gene. The upregulation of *FT* could amplify the plant's ability to adapt to seasonal or environmental cues, such as light or temperature changes, ensuring reproductive success in fluctuating environments. This observation underscores the intricate connection between genetic mutations, hormonal signaling pathways and the timing of key developmental transitions like flowering.

MATERIALS AND METHODS

Plant material and growth conditions In this experiment, we utilized Col-0 and L*er* accessions of wild-type Arabidopsis. The *hy2* (*SALK_104923C*) and *nrpd1a-3* (*CS66150*) mutants, both in the Col-0 background, were sourced from the ABRC Stock Center. Additionally, we generated a line by backcrossing the *hyo1* mutant with Col-0 twice. Seeds underwent sterilization by immersion in a chlorine bleach solution with 0.04% Triton X-100 for 5 min, followed by five rinses with sterile water. The sterilized seeds were then sown on 1/2 Murashige and Skoog (MS) medium containing 0.01% agarose, cold-treated in the dark at 4 °C for 2–3 days, and subsequently transferred to an incubator set at 21 °C, where they were grown under continuous light.

Heat stress condition To induce transgenerational transposition of *ONSEN*, *nrpd1* mutant seedlings, 7 days post-germination, were subjected to heat stress at 37 °C for 24 h. Seeds collected from these heat-stressed *nrpd1* plants were subsequently sown on 1/2 MS plates, cold-treated in the dark at 4 °C for 2 days, and then transferred to 21 °C. Phenotypic analysis was conducted under continuous light conditions to observe the resulting characteristics.

Measurement of hypocotyl length Seeds were sown on vertical 1/2 MS plates and subjected to a low-temperature treatment in the dark at 4 °C for 2 days. Following this treatment, the plates were transferred to 21 °C under continuous light. Hypocotyl lengths of seedlings were measured on the 5th day after germination, to assess phenotypic variation.

Mapping DNA was extracted from F2 plants derived from crosses between *hyo1* and L*er*, selecting individuals that exhibited the hypocotyl elongation phenotype. PCR analysis was performed using SSLP (simple sequence length polymorphism) markers to assess genetic associations, allowing us to estimate the chromosomal location of the gene responsible for this phenotype. Mapping primers, including NGA primers, are listed in Supplementary Table S1.

DNA sequencing PCR was performed using primers corresponding to the *HY2* and *ONSEN* regions for FASMAC premix analysis (FASMAC, Kanagawa, Japan).

qRT-PCR Total RNA was extracted from seedlings grown on 1/2 MS medium under continuous light using TRI Reagent (Sigma-Aldrich, St. Louis, MO, USA). For expression analysis, samples collected 7 days after germination were used to analyze *HY2*, while samples collected 8 days after germination were used to analyze *FT*. Post-extraction, RNA was treated with RQ1 RNase-Free DNase (Promega, Madison, WI, USA) and then reverse-transcribed into cDNA using the ReverTra Ace qPCR RT Kit (TOYOBO, Osaka, Japan). qPCR was performed on an Applied Biosystems 7300 Real-Time PCR System using Luna Universal qPCR Master Mix (New England BioLabs, Ipswich, MA, USA). Three biological repetitions were performed, and standard deviation was determined. Expression levels were determined using the Ct method. 18S rRNA was used as an internal control for the analysis of the *HY2* gene, while *ACT2* was used as the internal control for the analysis of the *FT* gene. qPCR amplification was carried out using the appropriate primers as listed in Supplementary Table S1.

We thank Ms. Xiaoying Niu for her guidance on the *ONSEN* transposition induction experiments and overall molecular genetic experiments. This work was supported by the JSPS International Joint Research Program (International Joint Research Acceleration Fund, Type A) Grant Number JP 21KK0263.

REFERENCES

Biémont, C., and Vieira, C. (2006) Genetics: junk DNA as an evolutionary force. Nature **443**, 521–524. DOI: 10.1038/443521a

Bucher, E., Reinders, J., and Mirouze, M. (2012) Epigenetic control of transposon transcription and mobility in *Arabidopsis*. Curr. Opin. Plant Biol. **15**, 503–510. DOI: 10.1016/j.pbi.2012.08.006

Casacuberta, E., and González, J. (2013) The impact of transposable elements in environmental adaptation. Mol. Ecol. **22**, 1503–1517. DOI: 10.1111/mec.12170

Cavrak, V. V., Lettner, N., Jamge, S., Kosarewicz, A., Bayer, L. M., and Scheid, O. M. (2014) How a retrotransposon exploits the plant's heat stress response for its activation. PLoS Genet. **10**, e1004115. DOI: 10.1371/journal.pgen.1004115

Contreras-Garrido, A., Galanti, D., Movilli, A., Becker, C., Bossdorf, O., Drost, H.-G., and Weigel, D. (2024) Transposon dynamics in the emerging oilseed crop *Thlaspi arvense*. PLoS Genet. **20**, e1011141. DOI: 10.1371/journal.pgen.1011141

Fultz, D., Choudury, S. G., and Slotkin, R. K. (2015) Silencing of active transposable elements in plants. Curr. Opin. Plant Biol. **27**, 67–76. DOI: 10.1016/j.pbi.2015.05.027

Gao, Z., Liu, H.-L., Daxinger, L., Pontes, O., He, X., Qian, W., Lin, H., Xie, M., Lorkovic, Z. J., Zhang, S., et al. (2010) An RNA polymerase II- and AGO4-associated protein acts in RNA-directed DNA methylation. Nature **465**, 106–109. DOI: 10.1038/nature09025

He, X., Qi, Z., Liu, Z., Chang, X., Zhang, X., Li, J., and Wang, M. (2024) Pangenome analysis reveals transposon-driven genome evolution in cotton. BMC Biol. **22**, 92. DOI: 10.1186/s12915-024-01893-2

Ito, H. (2022) Diversity and strategies of environmental stress-responsive transposons in plants. Genes Genet. Syst. **97**, 167. DOI: 10.1266/ggs.97.167

Ito, H., Gaubert, H., Bucher, E., Mirouze, M., Vaillant, I., and Paszkowski, J. (2011) An siRNA pathway prevents transgenerational retrotransposition in plants subjected to stress. Nature **472**, 115–159. DOI: 10.1038/nature09861

Ito, H., Kim, J.-M., Matsunaga, W., Saze, H., Matsui, A., Endo, T. A., Harukawa, Y., Takagi, H., Yaegashi, H., Masuta, Y., et al. (2016) A stress-activated transposon in *Arabidopsis* induces transgenerational abscisic acid insensitivity. Sci. Rep. **6**, 6:23181. DOI: 10.1038/srep23181

Kazazian, H. H., Jr (2004) Mobile elements: drivers of genome evolution. Science **303**, 1626–1632. DOI: 10.1126/science.1089670

Lisch, D. (2009) Epigenetic regulation of transposable elements in plants. Ann. Rev. Plant Biol. **60**, 43–66. DOI: 10.1146/annurev.arplant.59.032607.092744

Matsunaga, W., Kobayashi, A., Kato, A., and Ito, H. (2012) The effects of heat induction and the siRNA biogenesis pathway on the transgenerational transposition of *ONSEN*, a *copia*-like retrotransposon in *Arabidopsis thaliana*. Plant Cell Physiol. **53**, 824–833. DOI: 10.1093/pcp/pcr179

Matzke, M. A., and Birchler, J. A. (2005) RNAi-mediated pathways in the nucleus. Nat. Rev. Genet. **6**, 24–35. DOI: 10.1038/nrg1500

Sahebi, M., Hanafi, M. M., van Wijnen, A. J., Rice, D., Rafii, M. Y., Azizi, P., Osman, M., Taheri, S., Bakar, M. F. A., Isa, M. N. M., et al. (2018) Contribution of transposable elements

in the plant's genome. Gene **665**, 155–166. DOI: 10.1016/j.gene.2018.04.050

Wicker, T., Sabot, F., Hua-Van, A., Bennetzen, J. L., Capy, P., Chalhoub, B., Flavell, A., Leroy, P., Morgante, M., Panaud, O., et al. (2007) A unified classification system for eukaryotic transposable elements. Nat. Rev. Genet. **8**, 973–982. DOI: 10.1038/nrg2165

Wierzbicki, A. T., Haag, J. R., and Pikaard, C. S. (2008) Noncoding transcription by RNA polymerase Pol IVb/Pol V mediates transcriptional silencing of overlapping and adjacent genes. Cell **135**, 635–648. DOI: 10.1016/j.cell.2008.09.035